

# The “Resonances Via Padé” (RVP) Method

Ralf-Arno Tripolt, ECT\*, Trento, Italy

Based on arXiv: 1610.03252

Ralf-Arno Tripolt, Idan Haritan, Jochen Wambach, Nimrod Moiseyev

Gießen, December 7th, 2016

**ECT\***

EUROPEAN CENTRE FOR THEORETICAL STUDIES  
IN NUCLEAR PHYSICS AND RELATED AREAS

# Outline

---

## I) “Resonances Via Padé” (RVP) Method

- ▶ Definition and Properties

## II) Applications

- ▶ simple examples
- ▶ extraction of complex resonance poles and decay thresholds
- ▶ analytic continuation - from imaginary to real time

## III) Summary

# I) “Resonances Via Padé” (RVP) Method

$$\begin{aligned}
 S_p[\psi, \bar{\psi}, A] &= \sum_{n=0}^{\infty} \int d^6x \times \bar{\psi}^{(n)} \left[ \psi_{\mu} \partial_{\nu} + i g \left( \partial_{\mu} \psi \right) - m \right] \psi^{(n)} \rightarrow S_0[A] = \frac{i}{2\pi} \int d^6x T_{\mu\nu}^{\text{ext}}(A) F^{\mu\nu}(A) \\
 \psi(x) \mapsto \psi'(x) &= \Omega(x) \psi(x) \wedge \bar{\psi}'(x) \mapsto \bar{\psi}'(x) = \bar{\psi} \Omega^{\dagger}(x) \rightarrow S_0[\bar{\psi}, \bar{\psi}, A] = S_0[\psi, \bar{\psi}, A], S_2[m, \bar{\psi}, m] \\
 \Omega^{\dagger} \left[ \partial_{\mu} \left( \Omega \partial_{\mu} \psi \right) \right] &= \Omega^{\dagger} \left[ \left( \partial_{\mu} \Omega \right) \psi + \Omega \left( \partial_{\mu} \psi \right) \right] = \left[ \partial_{\mu} \Omega + \Omega^{\dagger} \Omega \partial_{\mu} \right] \psi = [\Omega^{\dagger} \partial_{\mu} \Omega + \partial_{\mu} \bar{\Omega}] \psi \\
 \bar{\psi} \Omega^{\dagger} \left( \partial_{\mu} + ig A_{\mu} \right) \Omega \psi &= \bar{\psi} \left( \partial_{\mu} + ig A_{\mu} \right) \psi \leftrightarrow S_2 \left[ \partial_{\mu} \left( \Omega \psi \right) + ig A_{\mu} (\Omega \psi) \right] = \partial_{\mu} \psi + ig A_{\mu} \psi \\
 \Rightarrow S_2 \left( \partial_{\mu} \Omega \right) \psi + i \Omega^{\dagger} \partial_{\mu} \psi &\leftrightarrow [\Omega^{\dagger} g A_{\mu} \Omega] \psi = \bar{\psi} \partial_{\mu} \psi + i \Omega^{\dagger} \Omega \partial_{\mu} \psi \\
 \Rightarrow A_{\mu} \rightarrow A_{\mu}^{\text{ext}} &= \Omega(x) A_{\mu}(x), S_2 \left( \partial_{\mu} \Omega \right) \Omega^{\dagger} \Omega \psi = S_2 \left( \partial_{\mu} \psi \right), D_{\mu} = \partial_{\mu} - ig A_{\mu}^{\text{ext}} \\
 D_{\mu} \rightarrow D_{\mu}^{\text{ext}} &= \partial_{\mu} + ig A_{\mu}(x) = \partial_{\mu} + ig A_{\mu}^{\text{ext}}(x), S_2 \left( \partial_{\mu} \Omega \right) \Omega^{\dagger} \Omega \psi = S_2 \left( \partial_{\mu} \psi \right), S_2 \left( \partial_{\mu} \psi \right) = \int d^6x T_{\mu\nu}^{\text{ext}}(A) F^{\mu\nu}(A) - A = \delta_{\mu\nu} \omega_{\nu}^{\text{ext}}, \omega_{\nu}^{\text{ext}} \\
 F_{\mu\nu} &\rightarrow F_{\mu\nu}^{\text{ext}} = S_2(x) F_{\mu\nu}(x) \\
 U_p(\omega) &\rightarrow U_{\text{ext}} = S_2(\omega)
 \end{aligned}$$


[courtesy L. Holicki]

# RVP Method - Definition

---

Given a finite set of  $N = M + 1$  real data points  $(\eta_i, F_i)$ , the aim is to find a function  $F(\eta)$  which represents the correct analytic continuation,

$$F(\eta) = \frac{P(\eta)}{Q(\eta)},$$

where  $P(\eta)$  and  $Q(\eta)$  are polynomials. We construct an analytical approximation to  $F(\eta)$  by using the Schlessinger point method

$$C_M(\eta) = \frac{F_1}{1 + \frac{z_1(\eta - \eta_1)}{1 + \frac{z_2(\eta - \eta_2)}{\ddots z_M(\eta - \eta_M)}}},$$

where the  $z_i$  are real coefficients chosen such that

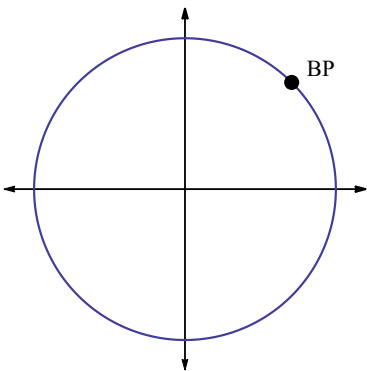
$$C_M(\eta_i) = F_i, \quad i = 1, 2, \dots, N.$$

An analytic continuation into the complex plane is performed by choosing  $\eta$  to be complex, i.e.  $\eta = \alpha e^{i\theta}$ .

# RVP Method - Radius of Convergence

---

- ▶ The radius of convergence of  $C_M(\eta)$  is given by the location of the nearest branch point in the complex plane
- ▶ the input points have to be chosen suitably, i.e. from the same analytic regime
- ▶ due to numerical uncertainties and the finite number of input points,  $C_M(\eta)$  can also give meaningful results beyond the BPs



## II) Applications

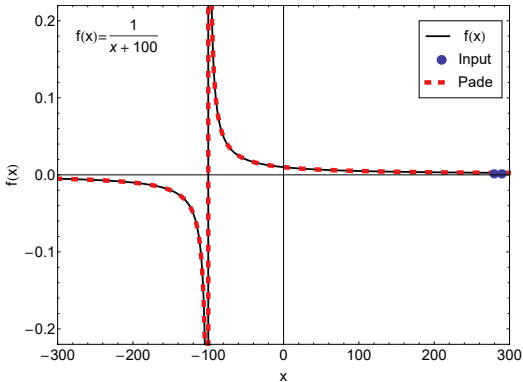
$S_p[\psi, \bar{\psi}, A] = \sum \int d^6x \times \bar{\psi}^{(1)} \left[ \gamma_5 (\partial_\mu + i g (\partial_\mu)^{(1)} + m^{(1)}) - \bar{\psi}^{(1)} \right] \rightarrow S[A] = \sum \int d^6x T \left[ F_{\mu\nu} A^\nu F^{\mu\nu} \right]$   
 $\psi(x) \mapsto \psi'(x) = D(x)\psi(x) \wedge \bar{\psi}(x) \mapsto \bar{\psi}'(x) = \bar{\psi}(x)D^\dagger(x) \rightarrow S[\psi, \bar{\psi}, A] = S[\psi', \bar{\psi}', A'] \cdot S^2 m^2 \delta = m$   
 $D^\dagger [\partial_\mu (\Sigma \psi)] = \Sigma^\dagger [(\partial_\mu \Sigma) \psi + \Sigma (\partial_\mu \psi)] = [\partial_\mu \Sigma + \Sigma^\dagger \Sigma \partial_\mu] \psi = [\partial_\mu \Sigma + \Sigma^\dagger \partial_\mu] \psi$   
 $\bar{\psi} D^\dagger (\partial_\mu + i g A_\mu) \Sigma \psi = \bar{\psi} (\partial_\mu + i g A_\mu) \psi \Leftrightarrow \Sigma^\dagger (\partial_\mu (\Sigma \psi) + i g A_\mu (\Sigma \psi)) = \partial_\mu \psi + i g A_\mu \psi$   
 $\Rightarrow \Sigma^\dagger (\partial_\mu \psi) + i g A_\mu \psi \Leftrightarrow [\Sigma^\dagger g A_\mu \Sigma] \psi = \partial_\mu \psi + i g A_\mu \psi \quad D_\mu = \partial_\mu - g A_\mu$   
 $\Rightarrow A_\mu \rightarrow A'_\mu = S(x) A_\mu$   
 $D_\mu \rightarrow D'_{\mu\nu} = \partial_\mu + i g A_\mu \delta_{\mu\nu}$   
 $F_{\mu\nu} \rightarrow F'_{\mu\nu} = S(x) F_{\mu\nu}$   
 $U_p(x) \rightarrow U_{p'}(x) = S(x)$ 


[courtesy L. Holicki]

# Simple Examples: $f(x) = 1/(x + 100)$

---

- ▶ Only 2 input points are needed to reconstruct  
 $f(x) = \frac{1}{x+100}$
- ▶ it is the “first guess” of the method

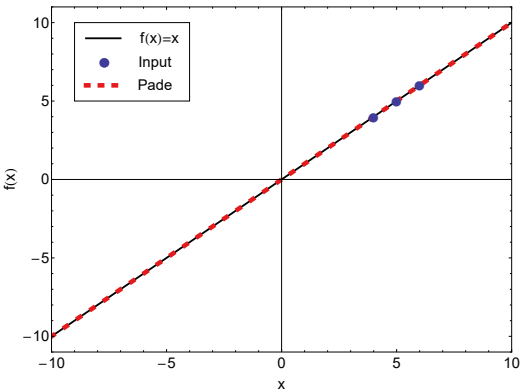


# Simple Examples: $f(x) = x$

---

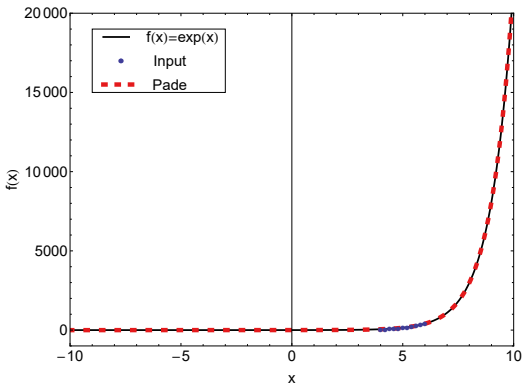
- ▶ 3 input points are needed to reconstruct  $f(x) = x$
- ▶ one obtains for example

$$C_M(x) = \frac{22 + 1.8 \cdot 10^{15}x}{1.8 \cdot 10^{15} - x} \approx x$$



# Simple Examples: $f(x) = e^x$

- ▶  $N \gtrsim 10$  input points are needed to obtain a reasonable reconstruction of  $f(x) = \exp(x)$

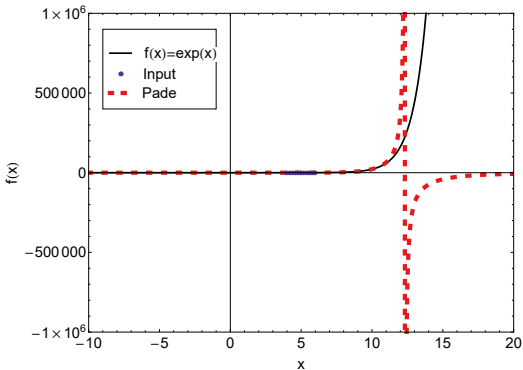


- ▶ for  $N = 11$  one obtains for example

$$C_M(x) = \frac{263504 + 170536x + 46451x^2 + 10389x^3 + 756x^4 + 148x^5}{265568 - 98809x + 15473x^2 - 1274x^3 + 55x^4 - x^5}$$

# Simple Examples: $f(x) = e^x$

- ▶  $N \gtrsim 10$  input points are needed to obtain a reasonable reconstruction of  $f(x) = \exp(x)$



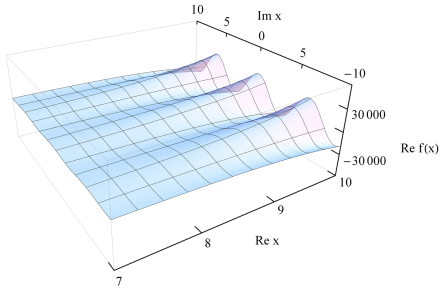
- ▶ for  $N = 11$  one obtains for example

$$C_M(x) = \frac{263504 + 170536x + 46451x^2 + 10389x^3 + 756x^4 + 148x^5}{265568 - 98809x + 15473x^2 - 1274x^3 + 55x^4 - x^5}$$

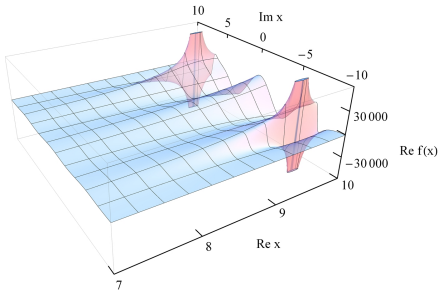
# Simple Examples: $f(x) = e^x$

---

$\operatorname{Re} \exp(x)$ :

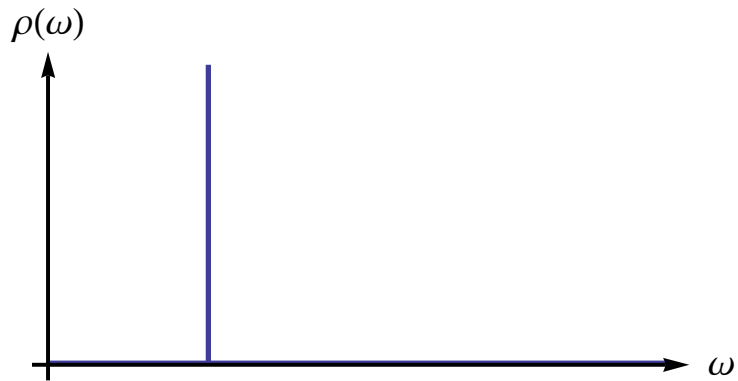


$\operatorname{Re} C_M(x)$ :



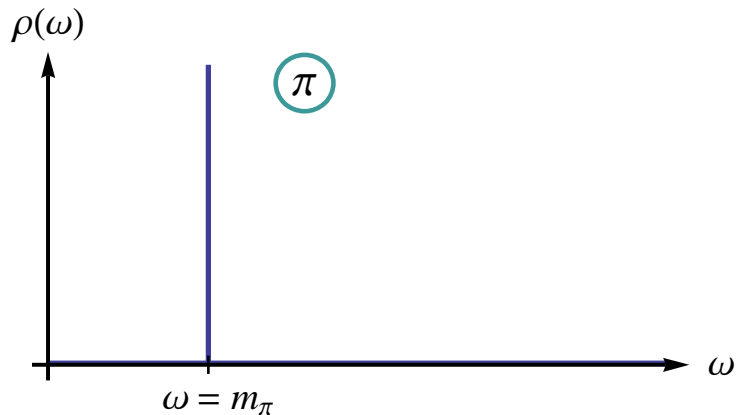
# What is a spectral function?

---



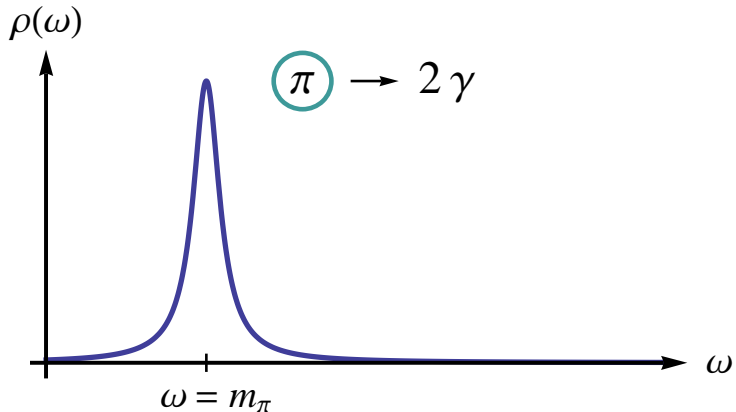
# What is a spectral function?

---

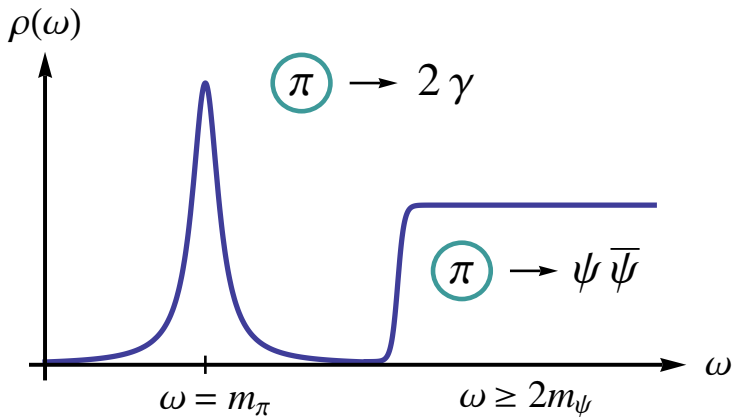


# What is a spectral function?

---



# What is a spectral function?



# Analytic example for a spectral function (I)

We use

$$\rho(\omega^2) = -\frac{1}{\pi} \text{Im} \left( \frac{1}{\omega^2 - M^2 - \Pi(\omega^2)} \right)$$

with the self energy

$$\Pi(\omega^2) = S_1 \log(T_1^2 - \omega^2) + S_2 \log(T_2^2 - \omega^2)$$

and the parameters

$$M = 50 \text{ MeV},$$

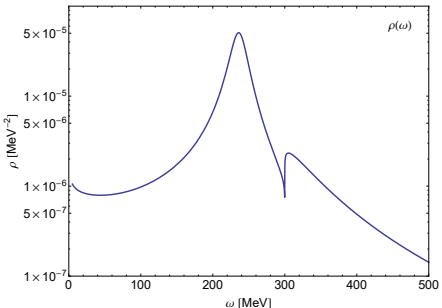
$$S_1 = 2000 \text{ MeV},$$

$$T_1 = 0 \text{ MeV},$$

$$S_2 = 3000 \text{ MeV},$$

$$T_2 = 300 \text{ MeV},$$

$$\omega \rightarrow \omega + i\varepsilon \text{ with } \varepsilon \rightarrow 0$$

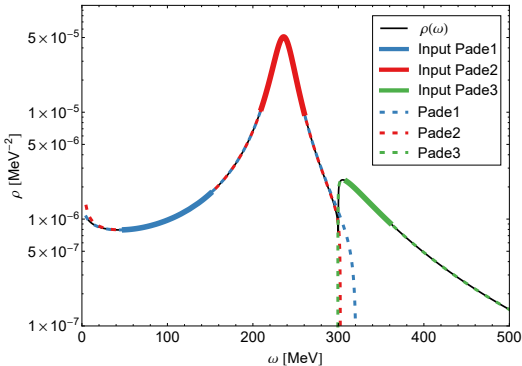


# Analytic example for a spectral function (II)

The decay thresholds at  $T_1 = 0$  MeV and  $T_2 = 300$  MeV represent branch points on the real axis.

Pade1 and Pade2 can be used to study the regime  $T_1 < \omega < T_2$ , Pade3 for  $\omega > T_2$ .

$N \approx 50$  input points were used for each regime.



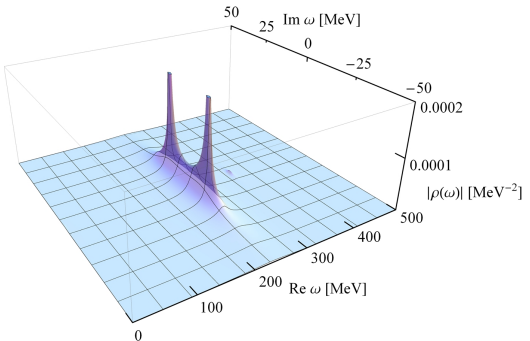
[R.-A. T., I. Haritan, J. Wambach and N. Moiseyev, arXiv:1610.03252]

# Analytic example for a spectral function (III)

The complex conjugate poles can be located by using Pade1 or Pade2:

$$\omega_P \approx (236.43 \pm i12.64) \text{ MeV}$$

The intrinsic error of the RVP method is usually negligible and here smaller than 0.01 MeV.



# Model for overlapping resonances (I)

We use the Kühn-Santamaria (KS) parametrization for the form factor

$$F(s) = \sum_{i=1}^3 \frac{M_i^2}{M_i^2 - s - i\Gamma_i \frac{M_i^2}{\sqrt{s}} \left( \frac{k(s)}{k(M_i^2)} \right)^3}$$

with

$$k(s) = \frac{\sqrt{s}}{2} \sqrt{1 - 4m_\pi^2/s}$$

and the parameters

$$M_1 = 0.5 \text{ GeV},$$

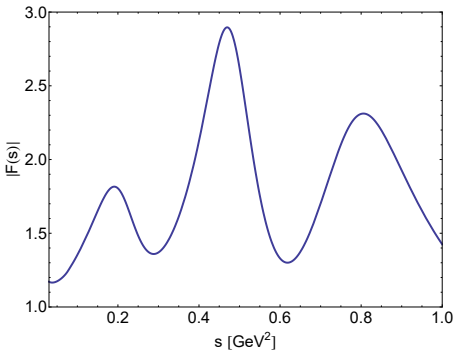
$$\Gamma_1 = 0.2 \text{ GeV},$$

$$M_2 = 0.7 \text{ GeV},$$

$$\Gamma_2 = 0.1 \text{ GeV},$$

$$M_3 = 0.9 \text{ GeV},$$

$$\Gamma_3 = 0.15 \text{ GeV},$$

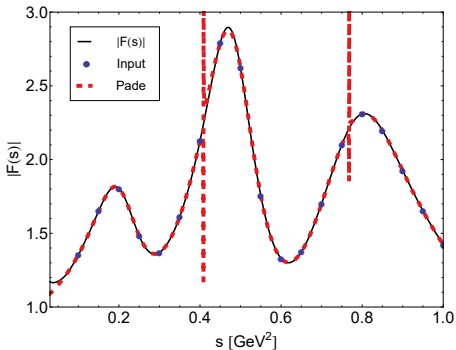


# Model for overlapping resonances (II)

$N = 19$  input points were used.

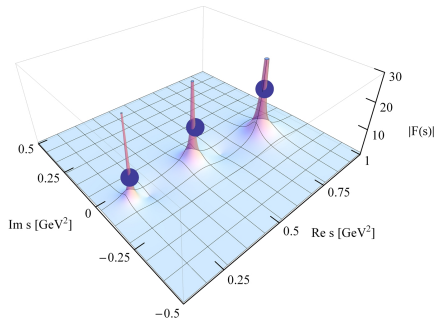
All resonance poles can be reconstructed at the same time since they are in the same analytic regime.

Additional poles can appear in the reconstruction, but they can be easily identified as being unphysical by varying the number of input points or the input region.

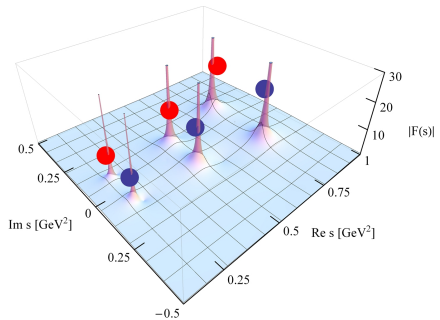


# Model for overlapping resonances (III)

exact result,  $F(s)$ :



reconstruction,  $C_M(s)$ :



# Model for strongly overlapping resonances (I)

We use the KS parametrization for the form factor

$$F(s) = \sum_{i=1}^3 \frac{M_i^2}{M_i^2 - s - i\Gamma_i \frac{M_i^2}{\sqrt{s}} \left( \frac{k(s)}{k(M_i^2)} \right)^3}$$

with

$$k(s) = \frac{\sqrt{s}}{2} \sqrt{1 - 4m_\pi^2/s}$$

and the parameters

$$M_1 = 0.5 \text{ GeV},$$

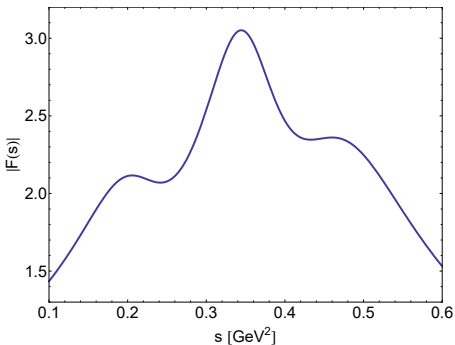
$$\Gamma_1 = 0.2 \text{ GeV},$$

$$M_2 = 0.6 \text{ GeV},$$

$$\Gamma_2 = 0.1 \text{ GeV},$$

$$M_3 = 0.7 \text{ GeV},$$

$$\Gamma_3 = 0.15 \text{ GeV},$$

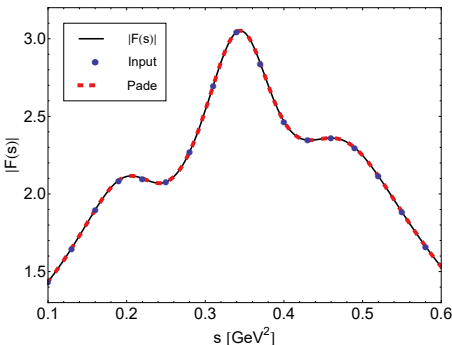


# Model for strongly overlapping resonances (II)

$N = 17$  input points were used.

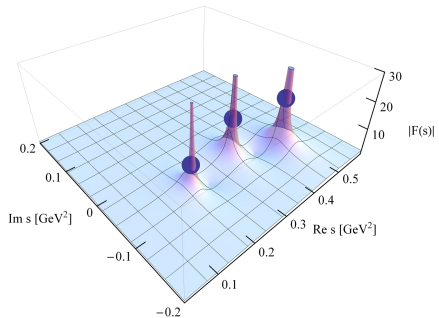
All resonance poles can be reconstructed at the same time since they are in the same analytic regime.

Additional poles can appear in the reconstruction, but they can be easily identified as being unphysical by varying the number of input points or the input region.

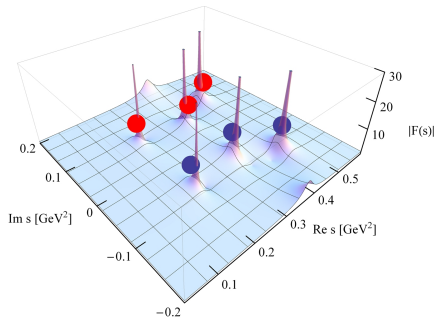


# Model for strongly overlapping resonances (III)

exact result,  $F(s)$ :



reconstruction,  $C_M(s)$ :

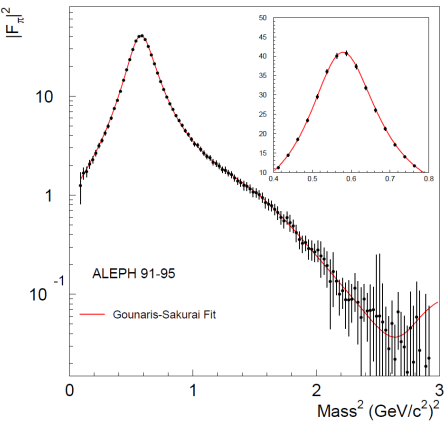


# Complex pole of the charged $\rho(770)$ meson

We use the RVP method to analyze the ALEPH data on the squared modulus of the  $\pi^-\pi^0$  vector form factor  $|F_\pi(s)|^2$ .

These data were obtained from  $\tau$ -lepton decays and represent the cleanest determination of the  $\rho(770)$ -meson mass and width.

$$\tau \rightarrow \pi^- \pi^0 \nu_\tau$$



[ALEPH collaboration, Phys. Rept. 421, 191-284, 2005,

arXiv:hep-ex/0506072]

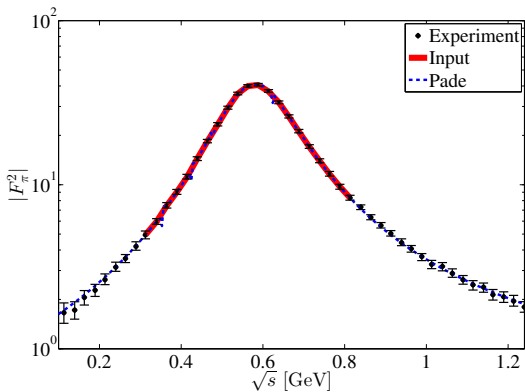
# Complex pole of the charged $\rho(770)$ meson

We use the RVP method to analyze the ALEPH data on the squared modulus of the  $\pi^-\pi^0$  vector form factor  $|F_\pi(s)|^2$ .

We find the complex pole of the charged  $\rho(770)$  meson to be at  $\sqrt{s_\rho} = M_\rho - i\Gamma_\rho/2$  with

$$M_\rho = 761.8 \pm 1.9 \text{ MeV},$$

$$\Gamma_\rho = 139.8 \pm 3.6 \text{ MeV}.$$



[R.-A. T., I. Haritan, J. Wambach and N. Moiseyev, arXiv:1610.03252]

# Complex pole of the charged $\rho(770)$ meson

We use the RVP method to analyze the ALEPH data on the squared modulus of the  $\pi^-\pi^0$  vector form factor  $|F_\pi(s)|^2$ .

We find the complex pole of the charged  $\rho(770)$  meson to be at  $\sqrt{s_\rho} = M_\rho - i\Gamma_\rho/2$  with

$$M_\rho = 761.8 \pm 1.9 \text{ MeV},$$

$$\Gamma_\rho = 139.8 \pm 3.6 \text{ MeV}.$$

$M_\rho$ (MeV)	$\Gamma_\rho$ (MeV)	source
$762.5 \pm 2$	$142 \pm 7$	[12]
$758.3 \pm 5.4$	$145.1 \pm 6.3$	[13]
$764.1 \pm 2.7^{+4.0}_{-2.5}$	$148.2 \pm 1.9^{+1.7}_{-5.0}$	[14]
$754 \pm 18$	$148 \pm 20$	[15]
$763.0 \pm 0.2$	$139.0 \pm 0.5$	[16]
$760 \pm 2$	$147 \pm 6$	[17]
$761 \pm 1$	$139 \pm 2$	[18]
$763.7 \pm 1.2$	$144 \pm 3$	[19]
$761.8 \pm 1.9$	$139.8 \pm 3.6$	this work

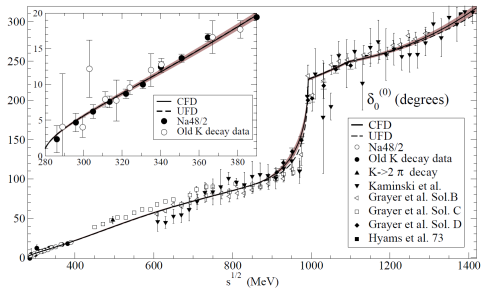
Table 1: Collection of pole parameter predictions for the  $\rho(770)$  meson.

[R.-A. T., I. Haritan, J. Wambach and N. Moiseyev, arXiv:1610.03252]

# Complex pole of the $f_0(500)$ or $\sigma$ meson

Locating the resonance pole is particularly difficult for the  $f_0(500)$  or  $\sigma$  meson due to its large decay width and the strong overlap with the background and higher resonances.

Plot: S0 wave phase shift for  $\pi\pi$ -scattering experimental data together with the UFD and CFD parameterizations.

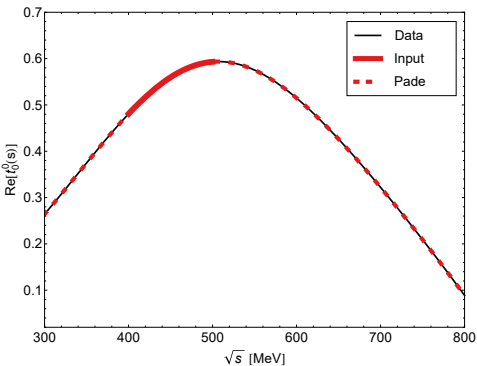


[R. Garcia-Martin, R. Kaminski, J. Pelaez, J. Ruiz de Elvira, and F. Yndurain, Phys.Rev. D83, 074004 (2011), arXiv:1102.2183 [hep-ph]]

# Complex pole of the $f_0(500)$ or $\sigma$ meson

We apply the RVP method to the real part of the S0 partial wave amplitude  $t_0^0(s)$  as obtained from the Constrained Fit to Data (CFD) parametrization of the  $\delta_0^{(0)}(s)$  phase shift,

$$t_0^0(s) = \frac{\eta_0^0(s)e^{2i\delta_0^0(s)} - 1}{2i\rho_\pi(s)}$$



[R.-A. T., I. Haritan, J. Wambach and N. Moiseyev, arXiv:1610.03252]

We find the complex pole at  $\sqrt{s_\sigma} = 450.1 \pm 11.2 - i(299.2 \pm 12.2)$  MeV

# Complex pole of the $f_0(500)$ or $\sigma$ meson

$\sqrt{s_\sigma}$ (MeV)	source
$470 \pm 30 - i(295 \pm 20)$	[24]
$470 \pm 50 - i(285 \pm 25)$	[16]
$441_{-8}^{+16} - i(272_{-12.5}^{+9})$	[25]
$457_{-13}^{+14} - i(279_{-7}^{+11})$	[26]
$442_{-8}^{+5} - i(274_{-5}^{+6})$	[27]
$453 \pm 15 - i(297 \pm 15)$	[28]
$449_{-16}^{+22} - i(275 \pm 12)$	[20]
$450.1 \pm 11.2 - i(299.2 \pm 12.2)$	this work

Table 3: Collection of pole parameter predictions for the  $f_0(500)$  or  $\sigma$  meson.

[R.-A. T., I. Haritan, J. Wambach and N. Moiseyev,

arXiv:1610.03252]

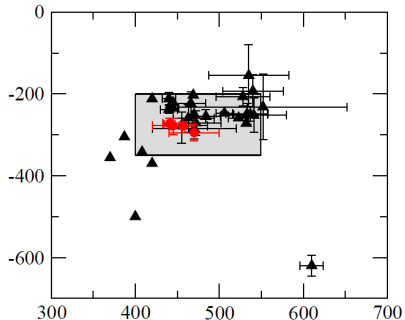


**Figure 1:** Location of the  $f_0(500)$  (or  $\sigma$ ) poles in the complex energy plane. Circles denote the recent analyses based on Roy(-like) dispersion relations [8–11], while all other analyses are denoted by triangles. The corresponding references are given in the listing.

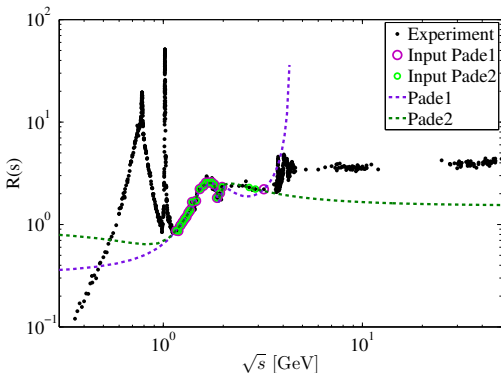
[K.A. Olive et al. (Particle Data Group), Chin. Phys. C38, 090001 (2014) (URL: <http://pdg.lbl.gov>)]

# Prediction of decay thresholds for $e^+e^-$ annihilation

We apply the RVP method to data on the ratio  $R(s)$  between the total cross sections of  $e^+e^-$  into hadrons and into muons,

$$R(s) = \frac{\sigma(e^+e^- \rightarrow \text{hadrons})}{\sigma(e^+e^- \rightarrow \mu^+\mu^-)}$$

Locating the threshold at  $\sqrt{s} \approx 4$  GeV is difficult in the present case where the experimental data are noisy.



[R.-A. T., I. Haritan, J. Wambach and N. Moiseyev, arXiv:1610.03252]

# Analytic continuation of Euclidean data

---

The Euclidean propagator can be written similar to a Laplace transform

$$\begin{aligned} G^E(\tau) &= \int_{-\infty}^{\infty} e^{-\omega\tau} I(\omega) d\omega \\ &= \int_{-\infty}^{\infty} \frac{e^{-\omega\tau}}{1 + e^{-\beta\omega}} \rho(\omega) d\omega \end{aligned}$$

In momentum space we have

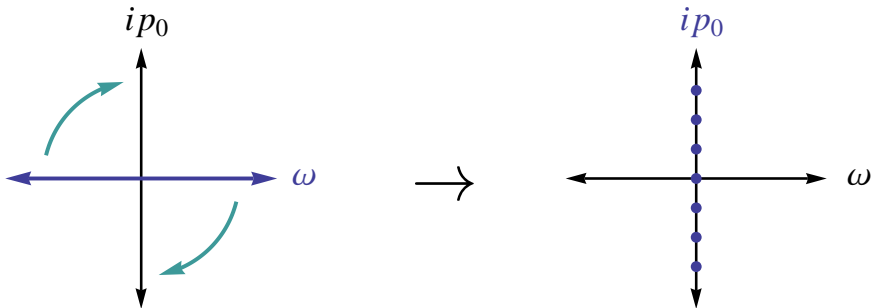
$$G^E(-ip_0) = \int_{-\infty}^{\infty} \frac{\rho(\omega)}{\omega + ip_0} d\omega$$

We will use the RVP method to perform an analytic continuation of  $\Gamma^{(2),E}(p_0) = 1/G^E(p_0)$  in order to obtain the real-time propagator  $G^R(\omega)$  and the spectral function,

$$\rho(\omega) = -\frac{1}{\pi} \text{Im} G^R(\omega) = \frac{1}{\pi} \frac{\text{Im} \Gamma^{(2),R}(\omega)}{(\text{Re} \Gamma^{(2),R}(\omega))^2 + (\text{Im} \Gamma^{(2),R}(\omega))^2}$$

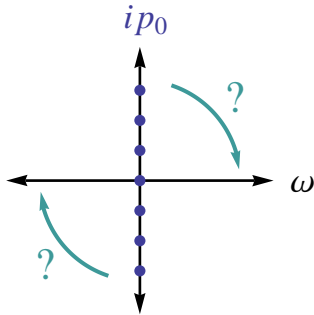
# The analytic continuation problem

Calculations at finite temperature are often performed using imaginary energies:



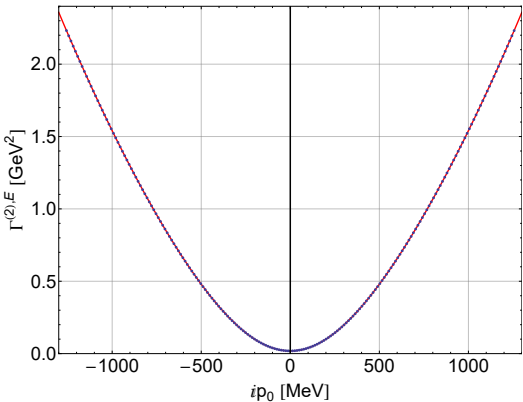
# The analytic continuation problem

Analytic continuation problem: How to get back to real energies?



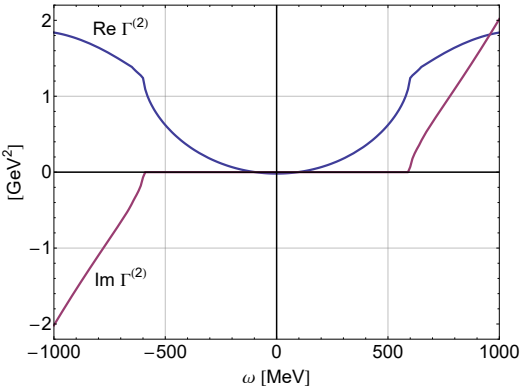
# Analytic continuation of Euclidean data

- ▶ We start from data on the Euclidean 2-point function  $\Gamma^{(2),E}(ip_0)$  for the pion at  $T = 2$  MeV
- ▶ The RVP method is used to obtain the analytic continuation  $\Gamma^{(2),R}(\omega)$



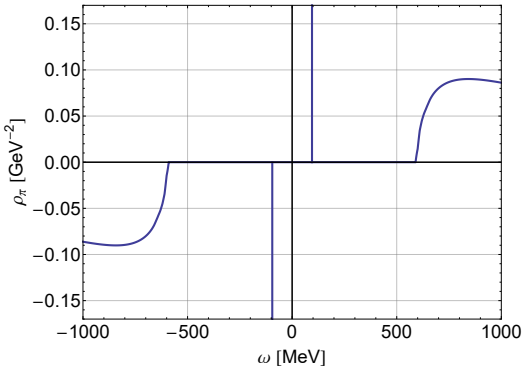
# Analytic continuation of Euclidean data

- ▶ the correct result for  $\Gamma^{(2),R}(\omega)$  is known and can be used to check the result obtained from the RVP method
- ▶  $\Gamma^{(2),R}(\omega)$  has a non-zero real and imaginary part as well as branch points due to the decay thresholds, in particular at  $\omega = 600$  MeV



# Analytic continuation of Euclidean data

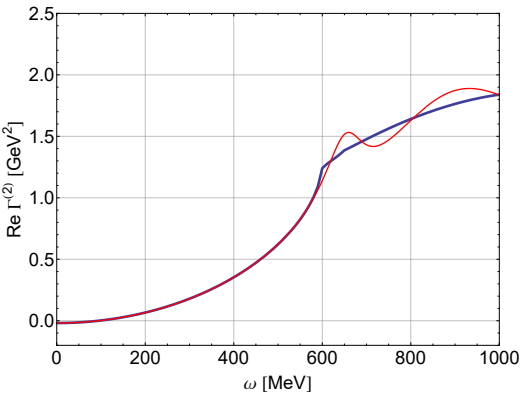
- ▶ the spectral function can be easily obtained from  $\Gamma^{(2),R}(\omega)$
- ▶ the branch point at  $\omega = 600 \text{ MeV}$  is clearly visible



$$\rho(\omega) = -\frac{1}{\pi} \text{Im} G^R(\omega) = \frac{1}{\pi} \frac{\text{Im} \Gamma^{(2),R}(\omega)}{(\text{Re} \Gamma^{(2),R}(\omega))^2 + (\text{Im} \Gamma^{(2),R}(\omega))^2}$$

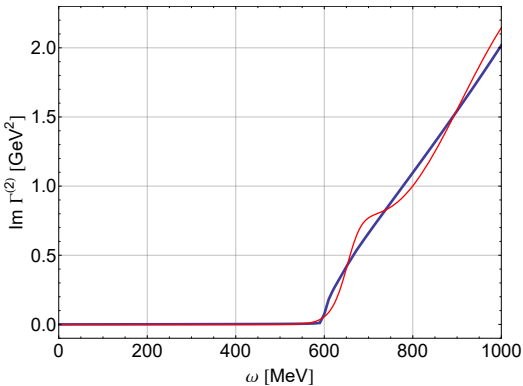
# Analytic continuation of Euclidean data

- ▶  $N = 65$  Euclidean input points between  $p_0 = 0$  MeV and  $p_0 = 2000$  MeV are used
- ▶ we can reproduce the low-energy part of  $\Gamma^{(2),R}(\omega)$  and also get a good estimate for energies beyond the branch point at  $\omega = 600$  MeV



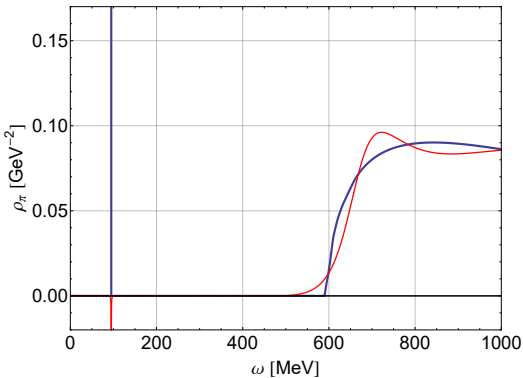
# Analytic continuation of Euclidean data

- ▶  $N = 65$  Euclidean input points between  $p_0 = 0$  MeV and  $p_0 = 2000$  MeV are used
- ▶ we can reproduce the low-energy part of  $\Gamma^{(2),R}(\omega)$  and also get a good estimate for energies beyond the branch point at  $\omega = 600$  MeV



# Analytic continuation of Euclidean data

- ▶  $N = 65$  Euclidean input points between  $p_0 = 0$  MeV and  $p_0 = 2000$  MeV are used
- ▶ we can reproduce the low-energy part of  $\Gamma^{(2),R}(\omega)$  and also get a good estimate for energies beyond the branch point at  $\omega = 600$  MeV



# Error analysis - $\sigma = 0$

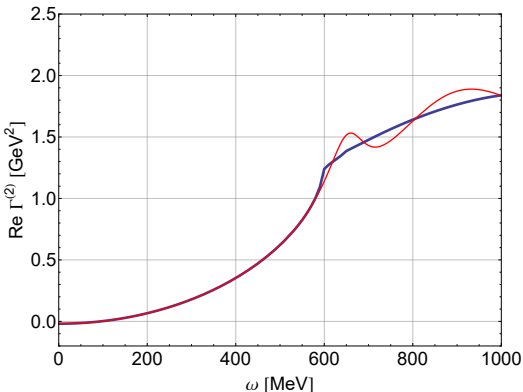
---

- ▶ We add Gaussian noise to the data:

$$f(x) = \frac{1}{\sqrt{2\pi}\sigma} e^{-\frac{(x-\mu)^2}{2\sigma^2}}$$

with  $\mu = y_i$  and  $\sigma = 0$

- ▶ Result for  $\text{Re } \Gamma^{(2),R}(\omega)$  when using  $N = 65$  Euclidean input points between  $p_0 = 0$  MeV and  $p_0 = 2000$  MeV:



# Error analysis - $\sigma = 10^{-7} \mu$

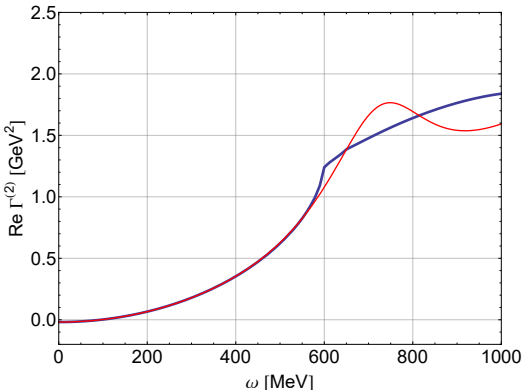
---

- ▶ We add Gaussian noise to the data:

$$f(x) = \frac{1}{\sqrt{2\pi}\sigma} e^{-\frac{(x-\mu)^2}{2\sigma^2}}$$

with  $\mu = y_i$  and  $\sigma = \mu/10^7$

- ▶ Result for  $\text{Re } \Gamma^{(2),R}(\omega)$  when using  $N = 65$  Euclidean input points between  $p_0 = 0$  MeV and  $p_0 = 2000$  MeV:



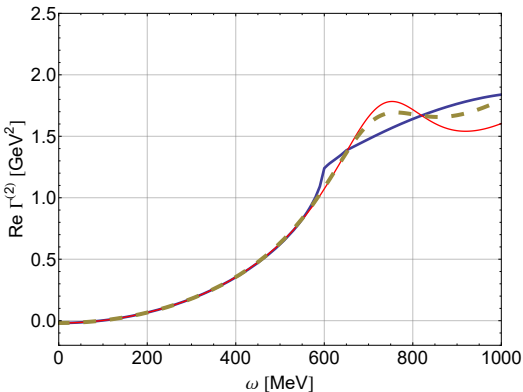
# Error analysis - $\sigma = 10^{-7}\mu$ - Smoothing

- We use a smoothing procedure after adding Gaussian noise to the data:

$$f(x) = \frac{1}{\sqrt{2\pi}\sigma} e^{-\frac{(x-\mu)^2}{2\sigma^2}}$$

with  $\mu = y_i$  and  $\sigma = \mu/10^7$

- Result for  $\text{Re } \Gamma^{(2),R}(\omega)$  when using  $N = 65$  Euclidean input points between  $p_0 = 0$  MeV and  $p_0 = 2000$  MeV:



# Error analysis - $\sigma = 10^{-6}\mu$

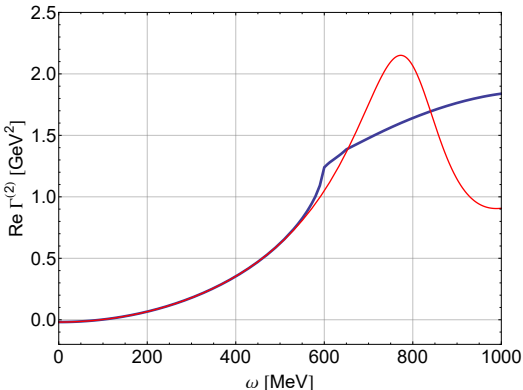
---

- ▶ We add Gaussian noise to the data:

$$f(x) = \frac{1}{\sqrt{2\pi}\sigma} e^{-\frac{(x-\mu)^2}{2\sigma^2}}$$

with  $\mu = y_i$  and  $\sigma = \mu/10^6$

- ▶ Result for  $\text{Re } \Gamma^{(2),R}(\omega)$  when using  $N = 65$  Euclidean input points between  $p_0 = 0$  MeV and  $p_0 = 2000$  MeV:



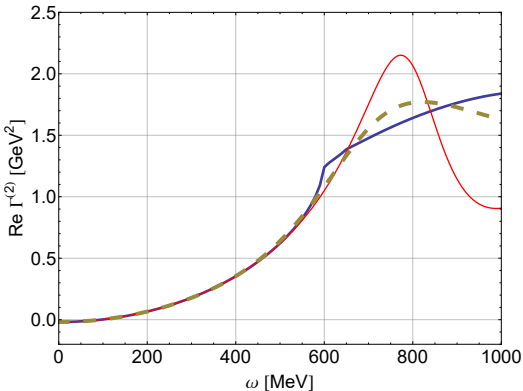
# Error analysis - $\sigma = 10^{-6}\mu$ - Smoothing

- ▶ We use a smoothing procedure after adding Gaussian noise to the data:

$$f(x) = \frac{1}{\sqrt{2\pi}\sigma} e^{-\frac{(x-\mu)^2}{2\sigma^2}}$$

with  $\mu = y_i$  and  $\sigma = \mu/10^6$

- ▶ Result for  $\text{Re } \Gamma^{(2),R}(\omega)$  when using  $N = 65$  Euclidean input points between  $p_0 = 0$  MeV and  $p_0 = 2000$  MeV:



# Error analysis - $\sigma = 10^{-5}\mu$

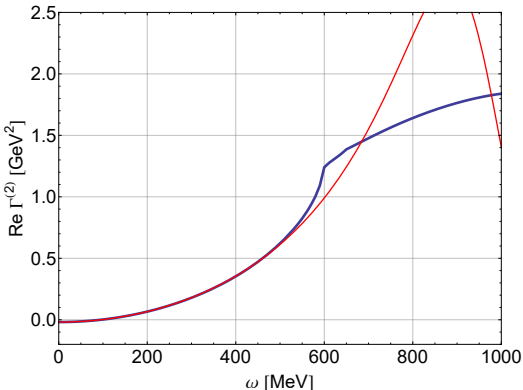
---

- ▶ We add Gaussian noise to the data:

$$f(x) = \frac{1}{\sqrt{2\pi}\sigma} e^{-\frac{(x-\mu)^2}{2\sigma^2}}$$

with  $\mu = y_i$  and  $\sigma = \mu/10^5$

- ▶ Result for  $\text{Re } \Gamma^{(2),R}(\omega)$  when using  $N = 65$  Euclidean input points between  $p_0 = 0$  MeV and  $p_0 = 2000$  MeV:



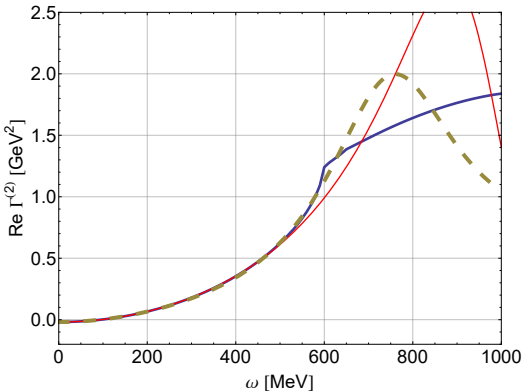
# Error analysis - $\sigma = 10^{-5}\mu$ - Smoothing

- ▶ We use a smoothing procedure after adding Gaussian noise to the data:

$$f(x) = \frac{1}{\sqrt{2\pi}\sigma} e^{-\frac{(x-\mu)^2}{2\sigma^2}}$$

with  $\mu = y_i$  and  $\sigma = \mu/10^5$

- ▶ Result for  $\text{Re } \Gamma^{(2),R}(\omega)$  when using  $N = 65$  Euclidean input points between  $p_0 = 0$  MeV and  $p_0 = 2000$  MeV:



# Error analysis - $\sigma = 0$

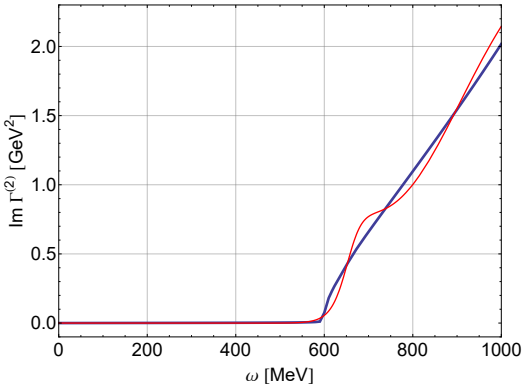
---

- ▶ We add Gaussian noise to the data:

$$f(x) = \frac{1}{\sqrt{2\pi}\sigma} e^{-\frac{(x-\mu)^2}{2\sigma^2}}$$

with  $\mu = y_i$  and  $\sigma = 0$

- ▶ Result for  $\text{Im } \Gamma^{(2),R}(\omega)$  when using  $N = 65$  Euclidean input points between  $p_0 = 0$  MeV and  $p_0 = 2000$  MeV:



# Error analysis - $\sigma = 10^{-7} \mu$

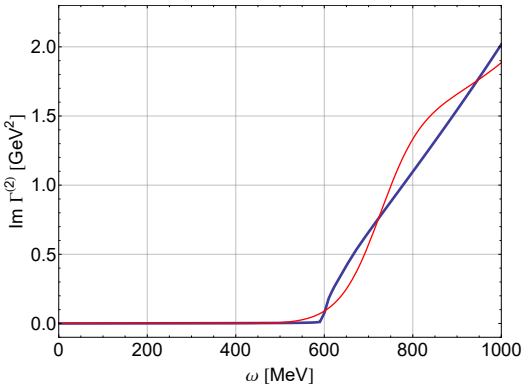
---

- ▶ We add Gaussian noise to the data:

$$f(x) = \frac{1}{\sqrt{2\pi}\sigma} e^{-\frac{(x-\mu)^2}{2\sigma^2}}$$

with  $\mu = y_i$  and  $\sigma = \mu/10^7$

- ▶ Result for  $\text{Im } \Gamma^{(2),R}(\omega)$  when using  $N = 65$  Euclidean input points between  $p_0 = 0$  MeV and  $p_0 = 2000$  MeV:



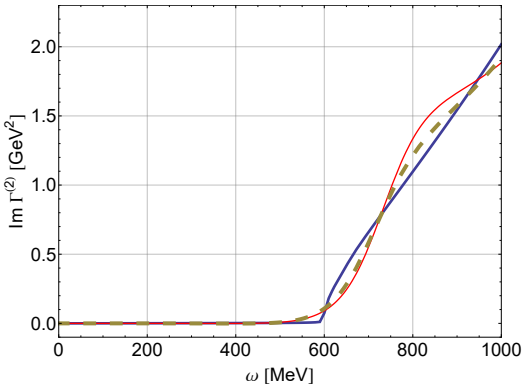
# Error analysis - $\sigma = 10^{-7}\mu$ - Smoothing

- ▶ We use a smoothing procedure after adding Gaussian noise to the data:

$$f(x) = \frac{1}{\sqrt{2\pi}\sigma} e^{-\frac{(x-\mu)^2}{2\sigma^2}}$$

with  $\mu = y_i$  and  $\sigma = \mu/10^7$

- ▶ Result for  $\text{Im } \Gamma^{(2),R}(\omega)$  when using  $N = 65$  Euclidean input points between  $p_0 = 0$  MeV and  $p_0 = 2000$  MeV:



# Error analysis - $\sigma = 10^{-6}\mu$

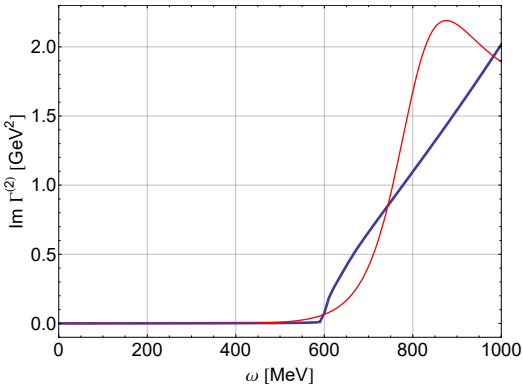
---

- ▶ We add Gaussian noise to the data:

$$f(x) = \frac{1}{\sqrt{2\pi}\sigma} e^{-\frac{(x-\mu)^2}{2\sigma^2}}$$

with  $\mu = y_i$  and  $\sigma = \mu/10^6$

- ▶ Result for  $\text{Im } \Gamma^{(2),R}(\omega)$  when using  $N = 65$  Euclidean input points between  $p_0 = 0$  MeV and  $p_0 = 2000$  MeV:



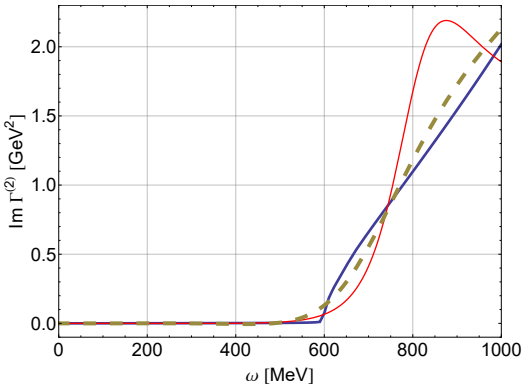
# Error analysis - $\sigma = 10^{-6}\mu$ - Smoothing

- We use a smoothing procedure after adding Gaussian noise to the data:

$$f(x) = \frac{1}{\sqrt{2\pi}\sigma} e^{-\frac{(x-\mu)^2}{2\sigma^2}}$$

with  $\mu = y_i$  and  $\sigma = \mu/10^6$

- Result for  $\text{Im } \Gamma^{(2),R}(\omega)$  when using  $N = 65$  Euclidean input points between  $p_0 = 0$  MeV and  $p_0 = 2000$  MeV:



# Error analysis - $\sigma = 10^{-5}\mu$

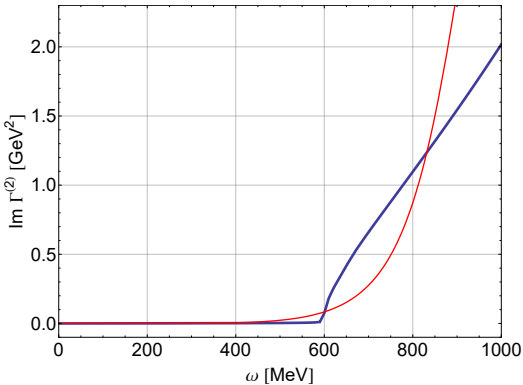
---

- ▶ We add Gaussian noise to the data:

$$f(x) = \frac{1}{\sqrt{2\pi}\sigma} e^{-\frac{(x-\mu)^2}{2\sigma^2}}$$

with  $\mu = y_i$  and  $\sigma = \mu/10^5$

- ▶ Result for  $\text{Im } \Gamma^{(2),R}(\omega)$  when using  $N = 65$  Euclidean input points between  $p_0 = 0$  MeV and  $p_0 = 2000$  MeV:



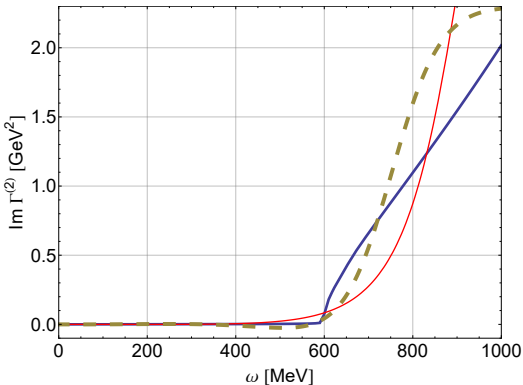
# Error analysis - $\sigma = 10^{-5}\mu$ - Smoothing

- We use a smoothing procedure after adding Gaussian noise to the data:

$$f(x) = \frac{1}{\sqrt{2\pi}\sigma} e^{-\frac{(x-\mu)^2}{2\sigma^2}}$$

with  $\mu = y_i$  and  $\sigma = \mu/10^5$

- Result for  $\text{Im } \Gamma^{(2),R}(\omega)$  when using  $N = 65$  Euclidean input points between  $p_0 = 0$  MeV and  $p_0 = 2000$  MeV:



# Error analysis - $\sigma = 0$

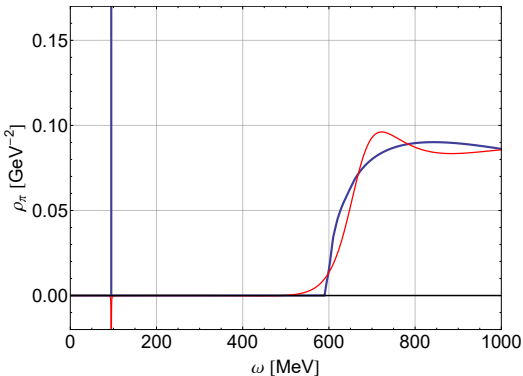
---

- ▶ We add Gaussian noise to the data:

$$f(x) = \frac{1}{\sqrt{2\pi}\sigma} e^{-\frac{(x-\mu)^2}{2\sigma^2}}$$

with  $\mu = y_i$  and  $\sigma = 0$

- ▶ Result for  $\rho(\omega)$  when using  $N = 65$  Euclidean input points between  $p_0 = 0$  MeV and  $p_0 = 2000$  MeV:



# Error analysis - $\sigma = 10^{-7} \mu$

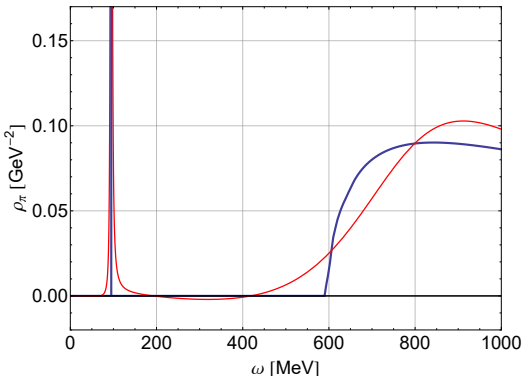
---

- ▶ We add Gaussian noise to the data:

$$f(x) = \frac{1}{\sqrt{2\pi}\sigma} e^{-\frac{(x-\mu)^2}{2\sigma^2}}$$

with  $\mu = y_i$  and  $\sigma = \mu/10^7$

- ▶ Result for  $\rho(\omega)$  when using  $N = 65$  Euclidean input points between  $p_0 = 0$  MeV and  $p_0 = 2000$  MeV:



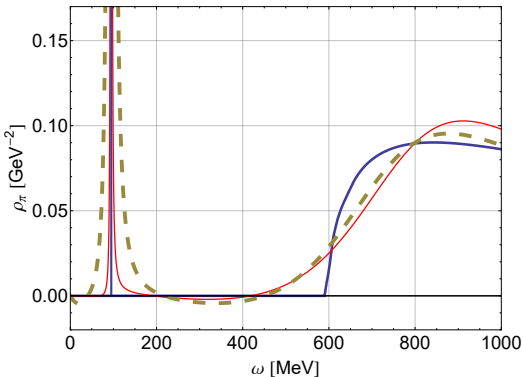
# Error analysis - $\sigma = 10^{-7}\mu$ - Smoothing

- ▶ We use a smoothing procedure after adding Gaussian noise to the data:

$$f(x) = \frac{1}{\sqrt{2\pi}\sigma} e^{-\frac{(x-\mu)^2}{2\sigma^2}}$$

with  $\mu = y_i$  and  $\sigma = \mu/10^7$

- ▶ Result for  $\rho(\omega)$  when using  $N = 65$  Euclidean input points between  $p_0 = 0$  MeV and  $p_0 = 2000$  MeV:



# Error analysis - $\sigma = 10^{-6}\mu$

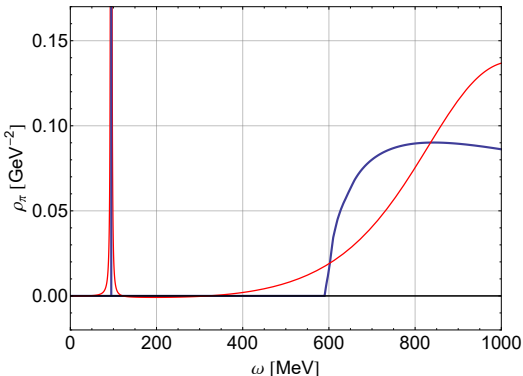
---

- ▶ We add Gaussian noise to the data:

$$f(x) = \frac{1}{\sqrt{2\pi}\sigma} e^{-\frac{(x-\mu)^2}{2\sigma^2}},$$

with  $\mu = y_i$  and  $\sigma = \mu/10^6$

- ▶ Result for  $\rho(\omega)$  when using  $N = 65$  Euclidean input points between  $p_0 = 0$  MeV and  $p_0 = 2000$  MeV:



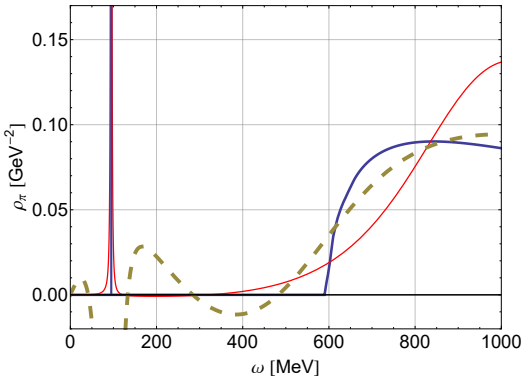
# Error analysis - $\sigma = 10^{-6}\mu$ - Smoothing

- We use a smoothing procedure after adding Gaussian noise to the data:

$$f(x) = \frac{1}{\sqrt{2\pi}\sigma} e^{-\frac{(x-\mu)^2}{2\sigma^2}}$$

with  $\mu = y_i$  and  $\sigma = \mu/10^6$

- Result for  $\rho(\omega)$  when using  $N = 65$  Euclidean input points between  $p_0 = 0$  MeV and  $p_0 = 2000$  MeV:



# Error analysis - $\sigma = 10^{-5}\mu$

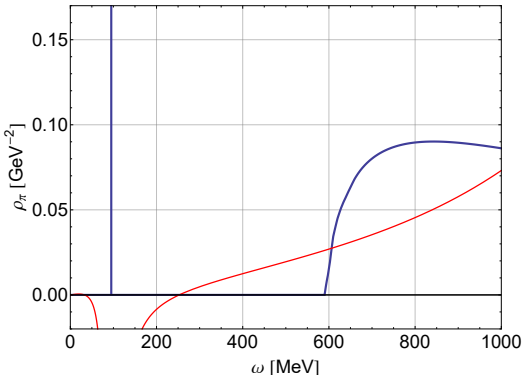
---

- ▶ We add Gaussian noise to the data:

$$f(x) = \frac{1}{\sqrt{2\pi}\sigma} e^{-\frac{(x-\mu)^2}{2\sigma^2}},$$

with  $\mu = y_i$  and  $\sigma = \mu/10^5$

- ▶ Result for  $\rho(\omega)$  when using  $N = 65$  Euclidean input points between  $p_0 = 0$  MeV and  $p_0 = 2000$  MeV:



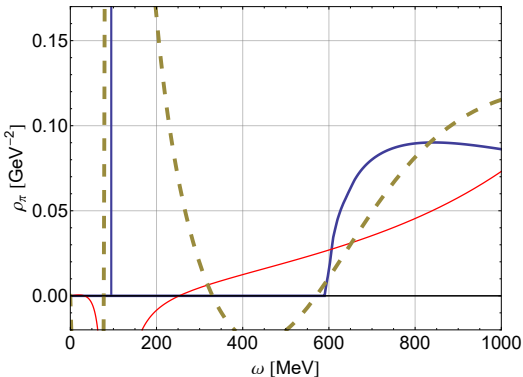
# Error analysis - $\sigma = 10^{-5}\mu$ - Smoothing

- We use a smoothing procedure after adding Gaussian noise to the data:

$$f(x) = \frac{1}{\sqrt{2\pi}\sigma} e^{-\frac{(x-\mu)^2}{2\sigma^2}}$$

with  $\mu = y_i$  and  $\sigma = \mu/10^5$

- Result for  $\rho(\omega)$  when using  $N = 65$  Euclidean input points between  $p_0 = 0$  MeV and  $p_0 = 2000$  MeV:



# Summary

---

We have introduced the Resonances Via Padé (RVP) method to obtain the analytic continuation of a function given in numerical form.

- ▶ only requires real input in order to reconstruct the underlying function not only along the real axis but also in the complex plane
- ▶ can be used to identify resonance poles and to predict decay thresholds
- ▶ can in principle be used to obtain real-time information starting from Euclidean data with small errors